

Quintom cosmology and modified gravity after DESI 2024

Yuhang Yang,^{1,2,3} Xin Ren,^{1,2,3,4} Qingqing Wang,^{1,2,3} Zhiyu Lu,^{1,2,3} Dongdong Zhang,^{1,2,3,5}
Yi-Fu Cai,^{1,2,3,*} and Emmanuel N. Saridakis^{6,2,7,†}

¹*Department of Astronomy, School of Physical Sciences,
University of Science and Technology of China, Hefei, Anhui 230026, China*

²*CAS Key Laboratory for Researches in Galaxies and Cosmology, School of Astronomy and Space Science,
University of Science and Technology of China, Hefei, Anhui 230026, China*

³*Deep Space Exploration Laboratory, Hefei 230088, China*

⁴*Department of Physics, Tokyo Institute of Technology, Tokyo 152-8551, Japan*

⁵*Kavli IPMU (WPI), UTIAS, The University of Tokyo, Kashiwa, Chiba 277-8583, Japan*

⁶*National Observatory of Athens, Lofos Nymfon, 11852 Athens, Greece*

⁷*Departamento de Matemáticas, Universidad Católica del Norte,
Avda. Angamos 0610, Casilla 1280 Antofagasta, Chile*

(Dated: May 1, 2024)

We reconstruct the cosmological background evolution under the scenario of dynamical dark energy through the Gaussian process approach, using the latest Dark Energy Spectroscopic Instrument (DESI) baryon acoustic oscillations (BAO) [1] combined with other observations. Our results reveal that the reconstructed dark-energy equation-of-state (EoS) parameter $w(z)$ exhibits the so-called quintom-B behavior, crossing -1 from phantom to quintessence regime as the universe expands. We investigate under what situation this type of evolution could be achieved from the perspectives of field theories and modified gravity. In particular, we reconstruct the corresponding actions for $f(R)$, $f(T)$, and $f(Q)$ gravity, respectively. We explicitly show that, certain modified gravity can exhibit the quintom dynamics and fit the recent DESI data efficiently, and for all cases the quadratic deviation from the Λ CDM scenario is mildly favored.

Keywords: DESI, quintom cosmology, modified gravity

Introduction – With the era of precision cosmology, our understanding on the evolution of the universe has greatly advanced. Astonishingly, the High Redshift Supernova Team [2] and the Supernova Cosmology Project [3] discovered that distant Type Ia supernovae (SN Ia) were accelerating away at an increasing pace, following which further evidence from the Cosmic Microwave Background (CMB) [4], BAO [5–7], and large-scale structure survey [8–10] confirmed the accelerating expansion as well. This led to the concept of dark energy, responsible for such a phenomenon, but the underlying nature remains mysterious. Facing to the aforementioned phenomenon, there are growing interests in various cosmological models. Despite of the simplest version of the cosmological constant Λ , there are many other candidate scenarios, namely dynamical dark energy models [11–13]. Some implementations of dynamical dark energy are known as scalar-field models, including quintessence [14, 15], phantom [16], quintom [17], K-essence [18, 19] and so on. The feature shared by all these models is a time-evolving EoS w . For quintessence, the value of w is always larger than -1 , while for phantom $w < -1$. Meanwhile, w can cross -1 , thereby enabling the description of a broader range of cosmological evolution in quintom cosmology [20–23]. To be specific, in the quintom-A scenario w is arranged to evolve from above -1 at early

times to below -1 at late times; while, in quintom-B w changes from the phantom phase to the quintessence phase as the universe expands. Note that, in general the realization of quintom-B is challenging when compared to quintom-A [24, 25].

It is worth mentioning that, some observations put hints on an existence of the negative-valued effective energy density of dark energy at high redshifts [26–30], which poses a challenge to the scalar field theory of dark energy, as it violates the null energy condition [25, 31, 32]. Theoretically, modified gravity [33] can be a framework to provide an alternative explanation for the above issue. Particularly, in modified gravity the additional terms relative to general relativity can behave as a component with the dynamical EoS, and thus can serve as an effective form of dynamical dark energy. One can develop curvature-based extended gravitational theories, such as $f(R)$ gravity [34–36]. Modified gravity theories can also be constructed based on other geometric gravity equivalent to general relativity. Starting from the torsion-based Teleparallel Equivalent of General Relativity, one can extend it to $f(T)$ gravity [37–40]. The extensions of Symmetric Teleparallel Equivalent of General Relativity based on non-metricity leads to $f(Q)$ gravity [41, 42]. These theories have been widely studied in cosmological frameworks [43–46].

Confronted with the landscape of theoretical upsurge such as the physical meaning of dark energy, and the gravitational descriptions underpinning the geometry of the universe, there is an urgent need for observational

*Electronic address: yifucai@ustc.edu.cn

†Electronic address: msaridak@noa.gr

guidance to steer the course of theoretical development. BAO data act as a powerful tool for probing cosmic distances, and play a pivotal role in the study of dark energy properties. Previous works had found implications of dynamical dark energy: 3.5σ evidence by using Bayesian Method with the data from SDSS DR7, BOSS and WiggleZ [47, 48]. Recently, the release of DESI provided measurements of the transverse comoving distance and Hubble rate, showing a possible tension with respect to the Λ CDM scenario at the level of 3.9σ [1]. Combining the DESI data with CMB and Supernova, provides indications of a deviation from a cosmological constant in favor of dynamical dark energy in [49]. Thus, confrontation with DESI data has attracted the interest of the community, suggesting interacting dark energy [50], quintessence scalar fields [51, 52], dark radiation [53], and other scenarios beyond Λ CDM paradigm [54–56]. In this work, we take full advantage of the most recent DESI data to reconstruct the dynamic evolution of our universe via the model-independent Gaussian process. We explain the quintom behavior of $w(z)$ within the framework of modifications of gravity, including $f(R)$, $f(T)$, and $f(Q)$ theories, then reconstruct the corresponding involved unknown function.

Dynamical evolution and quintom cosmology – BAO measurements are conducted across various redshift intervals, thereby enabling the imposition of constraints upon the cosmological parameters that regulate the distance-redshift relationship. The DESI BAO data includes tracers luminous red galaxy (LRG), emission line galaxies (ELG) and the Lyman- α forest (Ly α QSO) in a redshift range $0.1 \leq z \leq 4.2$ [57, 58]. The preliminary data includes quantities of $D_M(z)/r_d$, $D_H(z)/r_d$ and $D_V(z)/r_d$ within 7 distinct redshift bins. Here r_d is the drag-epoch sound horizon and the transverse comoving distance $D_M(z) = r_d/\Delta\theta$, equivalent distance $D_H(z) = c/H(z)$ and angle-average distance $D_V(z) = (zD_M^2(z)D_H(z))^{1/3}$. For later reconstruction we use the 5 $D_H(z)/r_d$ data and impose $r_d = 147.09 \pm 0.26$ Mpc [4] obtained from CMB to directly calibrating the BAO standard ruler.

To investigate the impact of the DESI data on the dark-energy EoS parameter, we consider three scenarios: in the first case, we exclusively utilize the distance data from DESI to reconstruct the evolution of the Hubble parameter with redshift. As a control sample, the second group consists solely of data from SDSS and WiggleZ, which serves to verify whether the results from DESI indeed provide stronger evidence for models featuring dynamical dark energy. For the third scenario, we combine the DESI data with complementary datasets [6, 59–61] from SDSS and WiggleZ, but in order to maximize the utility of the DESI observations, overlapping redshift measurements from other surveys are discarded where DESI data is available. All the samples we used including five DESI data and previous BAO (P-BAO) data are listed in Appendix A in Table III.

In order to reconstruct the history of cosmic dynam-

ics evolution from the BAO data, we perform a model-independent reconstruction of the Hubble parameter by using the Gaussian process. The Gaussian process is a stochastic procedure to acquire a Gaussian distribution over functions from observational data [62], which has been widely used for the function reconstruction in cosmology [63–73]. The distribution of the function at different redshifts is related by the covariance function with hyperparameters. We reconstruct the evolution function of $H(z)$ and its derivative through Gaussian Process in Python (GAPP) based on the exponential covariance function $k(x, x') = \sigma_f^2 e^{-(x-x')^2/(2l^2)}$, where the σ_f and l are the hyperparameters [74].

By applying the GAPP steps, we obtain the reconstructed $H(z)$ function which is depicted in Fig. 1. The black curve denotes the mean value of the reconstruction by using DESI and P-BAO data, while the light blue shaded zones indicate the allowed regions at 1σ confidence level. Furthermore, the Λ CDM model has been depicted with the dash line, imposing the best fit $H_0 = 68.53 \pm 0.62$ km s $^{-1}$ Mpc $^{-1}$ in [1]. One can read that, at low redshift it can fit the reconstruction result by using DESI and P-BAO data well, but at high redshift the differences are statistically significant, as the Λ CDM results are higher than those derived from reconstruction. Meanwhile, the mean values of the reconstructed $H(z)$ by using DESI or P-BAO only is also shown in the figure. We find that the value $H_0^{\text{DESI}} = 94.22 \pm 13.81$ km s $^{-1}$ Mpc $^{-1}$ which results from only DESI is too high to fit CMB or SNIa observations. This suggests that due to the limited number of BAO data points from DESI, there is an absence of information for low redshift bins. Moreover, we also acquire the H_0 values from the reconstruction processes for other two cases, which are $H_0^{\text{P-BAO}} = 63.08 \pm 2.94$ km s $^{-1}$ Mpc $^{-1}$, $H_0^{\text{DESI+P-BAO}} = 64.64 \pm 2.52$ km s $^{-1}$ Mpc $^{-1}$, respectively.

Surprisingly, we notice that the DESI data point around $z = 0.51$ is much higher than the range of 1σ allowed by the reconstruction result. Actually, the DESI data near $z = 0.51$ is 2.44σ away from the P-BAO only result and 2.42σ away from DESI + P-BAO. This unexpected phenomenon is also mentioned in [50, 55], and if it indeed arises from systematics, a possible explanation would be statistical fluctuations. Thus, in the future we may need more observational data at $z = 0.51$ to extract more precise results.

We then use the $H(z)$ function presented above to reconstruct the dark-energy EoS. Following the Friedmann equations, one can easily define the dark-energy EoS as

$$w = \frac{-2\dot{H} - 3H^2 - p_m}{3H^2 - \rho_m}, \quad (1)$$

where $c \equiv 8\pi G \equiv 1$ is adopted. ρ_m and p_m are the energy density and pressure of the matter sector (baryonic plus cold dark matter), assuming it to be a perfect fluid. One can easily find $\rho_m = 3H_0^3\Omega_{m0}(1+z)^3$ by using the continuity equation of matter $\dot{\rho}_m + 3H(\rho_m + p_m) = 0$,

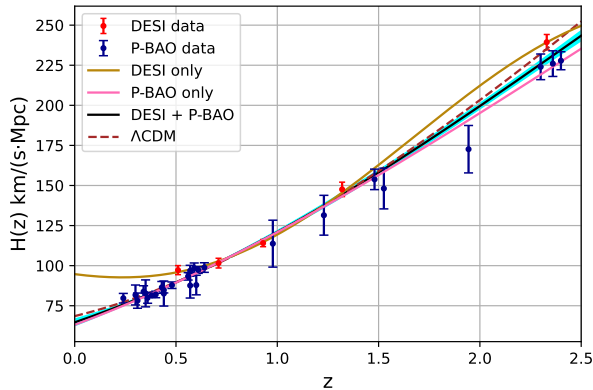


FIG. 1: The reconstructed $H(z)$ arising from DESI and P-BAO data through Gaussian process, without imposing the value of H_0 . The black curve denotes the mean value, while the light blue shaded zones indicate the allowed regions at 1σ confidence level for DESI + P-BAO. The dashed line corresponds to the Λ CDM scenario with the best fit value $H_0 = 68.53 \pm 0.62 \text{ km s}^{-1} \text{ Mpc}^{-1}$ of [1], while the mean value of the reconstructed $H(z)$ from DESI only or P-BAO only are additionally presented with the brown and pink curves respectively.

where $\Omega_{m0} = 0.3153 \pm 0.0073$ is the present value of the matter density parameter measured by Planck [4].

The reconstructed $w(z)$ for different data set is shown in Fig. 2. The mean values of $w(z)$ given by the three sets of data, all tend towards dynamical evolution. The results show that w has a tendency to cross zero for DESI data only, resulting from the divergence when the effective dark energy density crosses zero. For the result from P-BAO or the combined data, w exhibits a quintom-B behavior, which implies that it can cross -1 from the phantom phase to the quintessence phase. Further, we calculate the confidence of the quintom-B dynamics using the Monte Carlo simulation and obtain results of 0.93σ and 0.78σ for P-BAO only and DESI + P-BAO, which shall be better constrained by combining CMB and SN Ia data. The crossing redshift, in which w crosses -1 , is found to be 1.80, 2.18 for P-BAO only and DESI + P-BAO respectively, which indicate that the presence of DESI data can increase the value of w at high redshifts since the value of H at $z = 2.33$ from DESI is also larger than other data at the same redshift. It is worth noting that a similar quintom-B behavior of dark energy has also been found in previous articles [49], however the difference is that here we use BAO data to reconstruct w in a model-independent way, while in that work they used SN Ia data to perform the Monte Carlo Markov Chain method by assuming the evolution of w . Additionally, we find a different value for the crossing z . Meanwhile the results also show that Λ CDM scenario is beyond the 1σ allowed regions at low redshifts for both P-BAO only and DESI + P-BAO.

To fit the reconstruction result of w , we use the

parametrization, namely

$$w(z) = a + bz + cz^2 + dz^3, \quad (2)$$

where a, b, c, d are dimensionless parameters. The parameter values are presented in Table I, while the best fit curves are also shown in Fig. 2.

Data	P-BAO	DESI + P-BAO
a	-0.73	-0.78
b	0.13	0.10
c	0.10	0.23
d	-0.03	-0.11

TABLE I: The a, b, c and d dimensionless parameter values for best fitting, according to parametrization (2).

It is worth emphasizing that according to the “No-Go” theorem, the EoS parameters of a single scalar field is forbidden to cross -1 [25, 75, 76]. Therefore, this reconstruction results pose a significant challenge to the single scalar field dark energy model. The quintom model can be realized through various theories such as two scalar fields [77, 78], spinor fields [79], string theory [80], DHOST [81, 82] and Horndeski [83], more details are available in [25]. Due to the “No-Go” theorem, the explicit construction of the quintom scenario is more complex than that of other dynamical dark energy models. The realization of the quintom scenario requires a non-zero derivative of w near the crossing point. Also both the background and perturbations of scalar field must be stable and cross the boundary smoothly.

Meanwhile, the quintom model is widely used in the early universe. In a bouncing universe scenario, the universe initially contracts to a non-vanishing minimal radius before entering a subsequent phase of expansion. Following the bounce, as the universe transits into the hot Big Bang era, the EoS must shift from $w < -1$ to $w > -1$. This transition is characteristic of a quintom scenario [84, 85]. The quintom dynamics can also be utilized to realize cyclic cosmology [86] and emergent universe [87–89], potentially providing a solution to the singularity problem in the Big Bang cosmology.

One typical way to obtain a realization of the quintom-like phenomenon is within two scalar fields theory, if we combine one quintessence scalar field ϕ and one phantom scalar field σ . In such a case, the EoS parameter of quintom dark energy w_q can be written as

$$w_q = \frac{p_\phi + p_\sigma}{\rho_\phi + \rho_\sigma} = \frac{\frac{1}{2}\dot{\phi}^2 - V_\phi(\phi) - \frac{1}{2}\dot{\sigma}^2 - V_\sigma(\sigma)}{\frac{1}{2}\dot{\phi}^2 + V_\phi(\phi) - \frac{1}{2}\dot{\sigma}^2 + V_\sigma(\sigma)},$$

where $V_\phi(\phi)$, $V_\sigma(\sigma)$ are the potentials for each scalar field respectively. However, the appropriate potentials and initial conditions to realize the quintom behavior is quite difficult to be chosen. Nevertheless, since phantom scalar fields may exhibit problems at the quantum level [90,

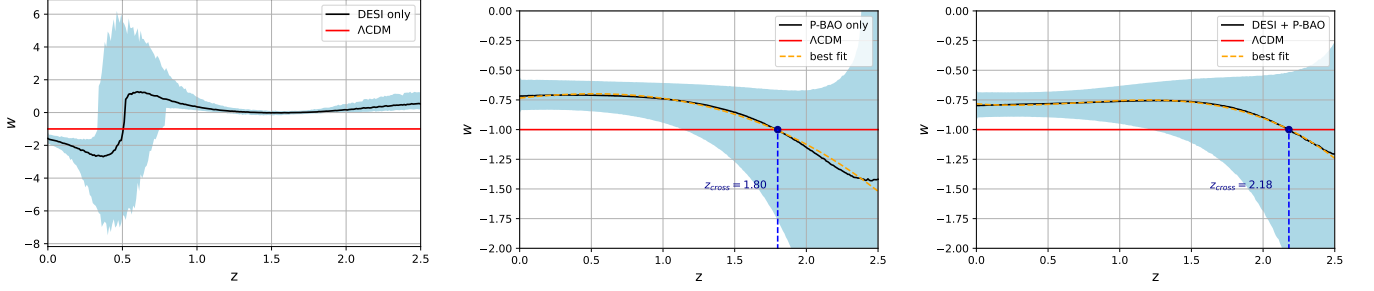


FIG. 2: The reconstructed dark-energy EoS parameter $w(z)$ for different datasets. The black curve denotes the mean value, while the light blue shaded zones indicate the allowed regions at 1σ confidence level. Additionally, we depict the best fit function $w(z) = a + bz + cz^2 + dz^3$, for P-BAO only data (where $a = -0.73, b = 0.13, c = -0.10, d = -0.03$) and for DESI + P-BAO data (where $a = -0.78, b = -0.10, c = 0.23, d = -0.11$). Finally, the red curve corresponds to the Λ CDM scenario in which $w = -1$. z_{cross} marks the point in which the phantom divide is crossed.

91], it would be more natural and simpler to explain the quintom behavior within modified gravity framework.

Gravitational reconstruction – For the gravitational reconstruction, we consider metric-affine gravity [92], describing gravity with a metric and a general affine connection. Such a general formulation can reduce to $f(R)$, $f(T)$, and $f(Q)$ gravity under certain conditions, based only on curvature, torsion or non-metricity respectively. These three metric-affine modified gravity theories constitute the geometric trinity of gravity. The action for curvature $f(R)$ gravity, torsional $f(T)$ gravity and non-metric $f(Q)$ gravity can be uniformly expressed as [36, 37, 41]

$$S = \int d^4x \sqrt{-g} \left[\frac{1}{2} f(X) + \mathcal{L}_m \right], \quad (3)$$

where X represents R, T or Q , with R, T, Q the Ricci scalar, torsion scalar and non-metricity scalar respectively. To apply these modified gravity theories in a cosmological framework, we consider the isotropic and homogeneous flat Friedmann-Robertson-Walker (FRW) metric $ds^2 = dt^2 - a(t)^2(dr^2 + r^2 d\theta^2 + r^2 \sin^2 \theta d\phi^2)$, with $a(t)$ the scale factor. The modified Friedmann equations can be expressed effectively as

$$\begin{aligned} 3H^2 &= \rho_m + \rho_{de}, \\ -2\dot{H} - 3H^2 &= p_m + p_{de}, \end{aligned} \quad (4)$$

where the effective energy density and pressure are in terms of the gravitational modifications.

In $f(R)$ gravity, we have

$$\begin{aligned} \rho_{de,R} &= \frac{1}{f_R} \left[\frac{1}{2} (f - Rf_R) - 3H\dot{R}f_{RR} \right], \\ p_{de,R} &= \frac{1}{f_R} (2H\dot{R}f_{RR} + \ddot{R}f_{RR}) \\ &\quad + \frac{1}{f_R} \left[\dot{R}^2 f_{RRR} - \frac{1}{2} (f - Rf_R) \right], \end{aligned} \quad (5)$$

where $R = -12H^2 - 6\dot{H}$ and $f_R = df/dR$, $f_{RR} = d^2f/dR^2$, and accordingly the effective dark-energy EoS is $w \equiv p_{de,R}/\rho_{de,R}$.

Similarly, in $f(T)$ gravity, we have the torsional energy density and pressure as

$$\begin{aligned} \rho_{de,T} &= -\frac{1}{2}F + TF_T, \\ p_{de,T} &= \frac{F - TF_T + 2T^2F_{TT}}{2 + 2F_T + 4TF_{TT}}, \end{aligned} \quad (6)$$

where we have introduced $f(T) = T + F(T)$ for convenience, and with $T = -6H^2$, and thus the effective dark-energy EoS parameter is $w \equiv p_{de,T}/\rho_{de,T}$. For $f(Q)$ gravity within coincident gauge, in the FRW metric at the background level, where $Q = -6H^2$, the corresponding expressions can be obtained from the one of $f(T)$ gravity, with the replacement $T \rightarrow Q$.

Since we have reconstructed the evolution of the dark-energy EoS parameter from the data, and we have expressed it in terms of the modified gravity involved function, based on $H(z)$ and its derivative we can straightforwardly obtain the reconstruction of these functions too. The details are provided in Appendix B. Then, from Eq. (B2) and Eq. (B5) we can reconstruct the evolution of $f(z)$ with $H(z)$ and $H'(z)$ in $f(X)$ cosmology. Afterwards, based on the relationship between X and $H(z)$, we can obtain f as the reconstructed function of X . The relation between $f(X)$ and X , using the reconstructed $H(z)$ results for P-BAO only and DESI + P-BAO from Fig. 1, are presented in Fig. 3. We mention that we do not use the DESI only result to obtain the reconstruction, since the $H(z)$ at low redshift does not behave very efficient. And we find the reconstruction results indicate $f(X)$ beyond the standard Λ CDM. In order to fit the reconstructed results of $f(X)$, we use the function form

$$F(X)/X_0 = A + BX/X_0 + CX^2/X_0^2, \quad (7)$$

where $F(X) = f(X) - X$ characterizes the derivation from general relativity, and A, B, C are dimensionless parameters with X_0 represents the value of X at current

time. Finally, in Table II we provide the parameter values for different metric-affine theories and different datasets. As we can see, in all cases, the quadratic deviation from Λ CDM scenario is mildly favoured by the data.

Model	$f(R)$		$f(T)$ or $f(Q)$	
Data	P-BAO	DESI + P-BAO	P-BAO	DESI + P-BAO
A	-0.601	-0.531	0.808	0.791
B	0.0342	0.00782	-0.0848	-0.0833
C	0.00391	0.00554	0.00261	0.000916

TABLE II: The best-fit parameter values for the modified gravity parametrization (7), namely for $f(R)$, $f(T)$, $f(Q)$ gravity with quadratic corrections.

Conclusion – The latest cosmological data released by DESI collaboration provides new insights for the exploration of the universe. In this work, we use the Hubble parameter data provided by DESI BAO and previous BAO observations to reconstruct the cosmological evolution of dynamical dark energy using Gaussian processes, which indicates a quintom-B dynamics for dark energy. Then we realize this scenario within modified gravity theories and reconstruct the corresponding action functions under the $f(R)$, $f(T)$, and $f(Q)$ frameworks.

As a first step we reconstruct the Hubble parameter $H(z)$ and the EoS parameter $w(z)$ for dynamical dark energy. We find that due to the lack of low-redshift information, the five BAO data points from DESI alone are insufficient to provide a complete picture of cosmic evolution. Additionally, the value of DESI data at $z = 0.51$ is beyond the 1σ allowed regions of the reconstructed $H(z)$ function. In particular, it is 2.44σ and 2.42σ away from the P-BAO only and DESI + P-BAO result, respectively. Interestingly, both P-BAO only and DESI + P-BAO datasets indicate that w exhibits a quintom-B behavior, crossing -1 from phantom to quintessence regime. The inclusion of data from DESI shifts the crossing point of w towards a higher redshift, namely from 1.80 to 2.18. The best fit function of the reconstructed w is also given. In order to explain such a quintom-B behavior, we choose the metric-affine modified gravity theory. Particularly, we derive the iterative relationship

of the function f with respect to z . Subsequently, the corresponding functions $f(R)$, $f(T)$, and $f(Q)$ can be obtained using the reconstruction results of $H(z)$ and its high-order derivatives. Furthermore, we provide the best fit functions, and in all cases the quadratic deviation from Λ CDM diagram is mildly favored. We conclude that these modified gravity theories can yield the dynamical dark energy scenarios inclined by BAO.

It has been 20 years since the conception of quintom dark energy was first proposed [17]. This nontrivial phenomenon indicate the potentially dynamical nature of the late-time cosmic acceleration which renew the understanding about our universe. Now the recent DESI data release seems to hint on the quintom-B behavior and challenge the Λ CDM paradigm. While accumulated observational data is expected to bolster the corresponding confidence level, this magnificent phenomenon already pave the way for observational tests of the quintom-B theoretical framework. Modified gravity or other possible theories as alternative mechanisms hold promise for being tested as well. Although current research is still far from conclusively deciding the nature of gravitational theory, our work fosters a bridge for future precise cosmological observations and theoretical mechanisms.

Acknowledgments

We are grateful to Pierre Zhang and Xinmin Zhang for insightful comments. This work is supported in part by National Key R&D Program of China (2021YFC2203100), by NSFC (12261131497, 12003029), by CAS young interdisciplinary innovation team (JCTD-2022-20), by 111 Project (B23042), by USTC Fellowship for International Cooperation, by USTC Research Funds of the Double First-Class Initiative. ENS acknowledges the contribution of the LISA CosWG and the COST Actions CA18108 “Quantum Gravity Phenomenology in the multi-messenger approach” and CA21136 “Addressing observational tensions in cosmology with systematics and fundamental physics (CosmoVerse)”. Kavli IPMU is supported by World Premier International Research Center Initiative (WPI), MEXT, Japan.

Appendix A: DESI and BAO data

In this Appendix, and in particular in Table III, we provide the Hubble parameter $H(z)$ used in this letter, obtained from DESI and previous BAO observations like SDSS and WiggleZ.

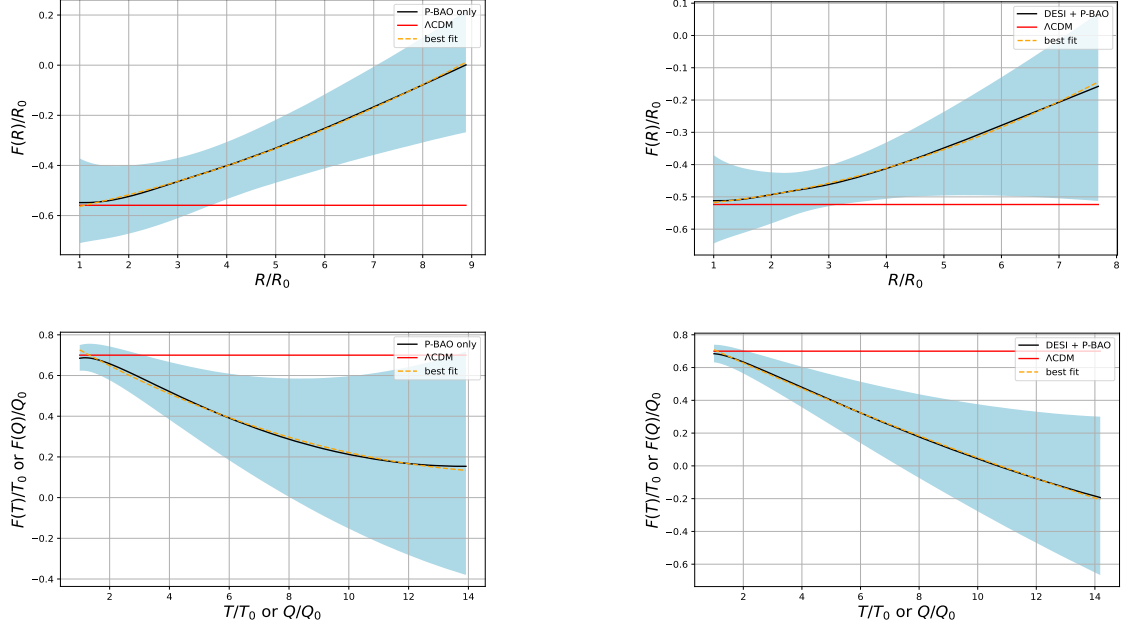


FIG. 3: The reconstructed $F(X)$ for different datasets, with $F(X) = f(X) - X$, where X represents R, T or Q , and with X_0 the current value. The black curve denotes the mean value, while the light blue shaded zones indicate the allowed regions at 1σ confidence level. The upper panels show the result of $F(R)$ gravity, while the lower panels show the result of $F(T)$ or $F(Q)$ gravity (since they coincide at the background level for FRW geometry within the coincident gauge). We use the parametrization (7), i.e. $F(X)/X_0 = A + BX/X_0 + CX^2/X_0^2$, to fit the reconstruction result, with the parameter values shown in Table II for P-BAO only and DESI + BAO data set, respectively. Additionally, the red line depicts the Λ CDM scenario, with $\Lambda^{P-BAO} = 0.7 \times 3H_0^2$ and $\Lambda^{DESI+P-BAO} = 0.7 \times 3H_0^2$.

Appendix B: Reconstruction method

In this Appendix we provide the details of the reconstruction procedure. In the case of $f(R)$ gravity we use the approximation

$$\begin{aligned} f_R &\equiv \frac{df(R)}{dR} = \frac{df/dz}{dR/dz} = \frac{f'}{R'} \\ f'(z) &\approx \frac{f(z + \Delta z) - f(z - \Delta z)}{2\Delta z} \\ f''(z) &\approx \frac{f(z + \Delta z) - f(z) + f(z - \Delta z)}{\Delta z^2}, \end{aligned} \quad (B1)$$

where f_R can be represented by $f(z)$ and $H(z)$. Furthermore, we can extract the recursive relation between the $f(z_{i+1})$, $f(z_i)$ and $f(z_{i-1})$ as

$$f(z_i + \Delta z) = \frac{\left(\frac{1}{2} + \frac{6H^2(-1-z)}{R'\Delta z^2}\right)f(z_i) + \left[\frac{3H^2 - \rho_m}{2R'\Delta z} + \frac{R}{4R'\Delta z} - \frac{3H^2(-1-z)}{R'\Delta z^2} + \frac{3H^2R''(-1-z)}{2R'^2\Delta z}\right]f(z_i - \Delta z)}{\frac{3H^2 - \rho_m}{2R'\Delta z} + \frac{R}{4R'\Delta z} + \frac{3H^2(-1-z)}{R'\Delta z^2} - \frac{3H^2R''(-1-z)}{2R'^2\Delta z}} \quad (B2)$$

where H is the value of the reconstructed $H(z)$ at z_i , $\Delta z = z_{i+1} - z_i = z_i - z_{i-1}$, and $\rho_m = \Omega_{m0} \times 3H_0^2(1 + z_i)^3$.

In the case of $f(T)$ gravity we perform the similar approximation

$$F_T \equiv \frac{dF(T)}{dT} = \frac{dF/dz}{dT/dz} = \frac{F'}{T'} \quad (B3)$$

$$F'(z) \approx \frac{F(z + \Delta z) - F(z)}{\Delta z}, \quad (B4)$$

Survey	Index	z_{eff}	$H(z) + \sigma_H$	Reference
DESI	1	0.51	97.21 ± 2.83	[1]
	2	0.71	101.57 ± 3.04	
	3	0.93	114.07 ± 2.24	
	4	1.32	147.58 ± 4.49	
	5	2.33	239.38 ± 4.80	
Previous BAO	6	0.24	79.69 ± 2.99	[93]
	7	0.30	81.70 ± 6.22	[94]
	8	0.31	78.17 ± 6.74	[95]
	9	0.34	83.17 ± 6.74	[93]
	10	0.35	82.70 ± 8.40	[96]
	11	0.36	79.93 ± 3.39	[95]
	12	0.38	81.50 ± 1.90	[5]
	13	0.40	82.04 ± 2.03	[95]
	14	0.43	86.45 ± 3.68	[93]
	15	0.44	82.60 ± 7.80	[97]
	16	0.44	84.81 ± 1.83	[95]
	17	0.48	87.79 ± 2.03	[95]
	18	0.56	93.33 ± 2.32	[95]
	19	0.57	87.60 ± 7.80	[10]
	20	0.57	96.80 ± 3.40	[98]
	21	0.59	98.48 ± 3.19	[95]
	22	0.60	87.90 ± 6.10	[97]
	23	0.61	97.30 ± 2.10	[5]
	24	0.64	98.82 ± 2.99	[95]
	25	0.978	113.72 ± 14.63	[99]
	26	1.23	131.44 ± 12.42	[99]
	27	1.48	153.81 ± 6.39	[100]
	28	1.526	148.11 ± 12.71	[99]
	29	1.944	172.63 ± 14.79	[99]
	30	2.30	224 ± 8	[101]
	31	2.36	226.0 ± 8.00	[102]
	32	2.40	227.8 ± 5.61	[103]

TABLE III: A list of BAO datasets used in this work, namely the values of $H(z)$ (in units of $\text{km s}^{-1}\text{Mpc}^{-1}$) and their errors σ_H at redshift z .

and thus we can acquire [63, 64]

$$F(z_i + \Delta z) = F(z_i) + 6\Delta z \frac{H'(z_i)}{H(z_i)} \cdot \left[H^2(z_i) - H_0^2 \Omega_{m0} (1 + z_i)^3 + \frac{F(z_i)}{6} \right]. \quad (\text{B5})$$

Finally, as mentioned above, for $f(Q)$ gravity we can change T to Q , since they share the same background evolution under the coincident gauge in FRW geometry.

[1] A. G. Adame, et al., DESI 2024 VI: Cosmological Constraints from the Measurements of Baryon Acoustic Oscillations (4 2024). [arXiv:2404.03002](#).

[2] A. G. Riess, et al., Observational evidence from supernovae for an accelerating universe and a cosmological constant, *Astron. J.* 116 (1998) 1009–1038. [arXiv:](#)

- [astro-ph/9805201](#).
- [3] S. Perlmutter, et al., Measurements of Ω and Λ from 42 High Redshift Supernovae, *Astrophys. J.* 517 (1999) 565–586. [arXiv:astro-ph/9812133](#).
 - [4] N. Aghanim, et al., Planck 2018 results. VI. Cosmological parameters, *Astron. Astrophys.* 641 (2020) A6, [Erratum: *Astron. Astrophys.* 652, C4 (2021)]. [arXiv:1807.06209](#).
 - [5] S. Alam, et al., The clustering of galaxies in the completed SDSS-III Baryon Oscillation Spectroscopic Survey: cosmological analysis of the DR12 galaxy sample, *Mon. Not. Roy. Astron. Soc.* 470 (3) (2017) 2617–2652. [arXiv:1607.03155](#).
 - [6] S. Alam, et al., Completed SDSS-IV extended Baryon Oscillation Spectroscopic Survey: Cosmological implications from two decades of spectroscopic surveys at the Apache Point Observatory, *Phys. Rev. D* 103 (8) (2021) 083533. [arXiv:2007.08991](#).
 - [7] K. T. Mehta, A. J. Cuesta, X. Xu, D. J. Eisenstein, N. Padmanabhan, A 2% Distance to $z = 0.35$ by Reconstructing Baryon Acoustic Oscillations - III : Cosmological Measurements and Interpretation, *Mon. Not. Roy. Astron. Soc.* 427 (2012) 2168. [arXiv:1202.0092](#).
 - [8] G. D’Amico, J. Gleyzes, N. Kokron, K. Markovic, L. Senatore, P. Zhang, F. Beutler, H. Gil-Marín, The Cosmological Analysis of the SDSS/BOSS data from the Effective Field Theory of Large-Scale Structure, *JCAP* 05 (2020) 005. [arXiv:1909.05271](#).
 - [9] M. M. Ivanov, M. Simonović, M. Zaldarriaga, Cosmological Parameters from the BOSS Galaxy Power Spectrum, *JCAP* 05 (2020) 042. [arXiv:1909.05277](#).
 - [10] C.-H. Chuang, et al., The clustering of galaxies in the SDSS-III Baryon Oscillation Spectroscopic Survey: single-probe measurements and the strong power of normalized growth rate on constraining dark energy, *Mon. Not. Roy. Astron. Soc.* 433 (2013) 3559. [arXiv:1303.4486](#).
 - [11] E. J. Copeland, M. Sami, S. Tsujikawa, Dynamics of dark energy, *Int. J. Mod. Phys. D* 15 (2006) 1753–1936. [arXiv:hep-th/0603057](#).
 - [12] G. Gubitosi, F. Piazza, F. Vernizzi, The Effective Field Theory of Dark Energy, *JCAP* 02 (2013) 032. [arXiv:1210.0201](#).
 - [13] P. Creminelli, F. Vernizzi, Dark Energy after GW170817 and GRB170817A, *Phys. Rev. Lett.* 119 (25) (2017) 251302. [arXiv:1710.05877](#).
 - [14] B. Ratra, P. J. E. Peebles, Cosmological Consequences of a Rolling Homogeneous Scalar Field, *Phys. Rev. D* 37 (1988) 3406.
 - [15] C. Wetterich, Cosmology and the Fate of Dilatation Symmetry, *Nucl. Phys. B* 302 (1988) 668–696. [arXiv:1711.03844](#).
 - [16] R. R. Caldwell, A Phantom menace?, *Phys. Lett. B* 545 (2002) 23–29. [arXiv:astro-ph/9908168](#).
 - [17] B. Feng, X.-L. Wang, X.-M. Zhang, Dark energy constraints from the cosmic age and supernova, *Phys. Lett. B* 607 (2005) 35–41. [arXiv:astro-ph/0404224](#).
 - [18] C. Armendariz-Picon, V. F. Mukhanov, P. J. Steinhardt, Essentials of k essence, *Phys. Rev. D* 63 (2001) 103510. [arXiv:astro-ph/0006373](#).
 - [19] M. Malquarti, E. J. Copeland, A. R. Liddle, M. Trodden, A New view of k-essence, *Phys. Rev. D* 67 (2003) 123503. [arXiv:astro-ph/0302279](#).
 - [20] J.-Q. Xia, B. Feng, X.-M. Zhang, Constraints on oscillating quintom from supernova, microwave background and galaxy clustering, *Mod. Phys. Lett. A* 20 (2005) 2409–2416. [arXiv:astro-ph/0411501](#).
 - [21] J.-Q. Xia, G.-B. Zhao, B. Feng, H. Li, X. Zhang, Observing dark energy dynamics with supernova, microwave background and galaxy clustering, *Phys. Rev. D* 73 (2006) 063521. [arXiv:astro-ph/0511625](#).
 - [22] G.-B. Zhao, J.-Q. Xia, M. Li, B. Feng, X. Zhang, Perturbations of the quintom models of dark energy and the effects on observations, *Phys. Rev. D* 72 (2005) 123515. [arXiv:astro-ph/0507482](#).
 - [23] Z.-K. Guo, Y.-S. Piao, X. Zhang, Y.-Z. Zhang, Two-Field Quintom Models in the w-w’ Plane, *Phys. Rev. D* 74 (2006) 127304. [arXiv:astro-ph/0608165](#).
 - [24] Y.-f. Cai, H. Li, Y.-S. Piao, X.-m. Zhang, Cosmic Duality in Quintom Universe, *Phys. Lett. B* 646 (2007) 141–144. [arXiv:gr-qc/0609039](#).
 - [25] Y.-F. Cai, E. N. Saridakis, M. R. Setare, J.-Q. Xia, Quintom Cosmology: Theoretical implications and observations, *Phys. Rept.* 493 (2010) 1–60. [arXiv:0909.2776](#).
 - [26] Y. Wang, L. Pogosian, G.-B. Zhao, A. Zucca, Evolution of dark energy reconstructed from the latest observations, *Astrophys. J. Lett.* 869 (2018) L8. [arXiv:1807.03772](#).
 - [27] K. Dutta, Ruchika, A. Roy, A. A. Sen, M. M. Sheikh-Jabbari, Beyond Λ CDM with low and high redshift data: implications for dark energy, *Gen. Rel. Grav.* 52 (2) (2020) 15. [arXiv:1808.06623](#).
 - [28] L. Visinelli, S. Vagnozzi, U. Danielsson, Revisiting a negative cosmological constant from low-redshift data, *Symmetry* 11 (8) (2019) 1035. [arXiv:1907.07953](#).
 - [29] S. Vagnozzi, New physics in light of the H_0 tension: An alternative view, *Phys. Rev. D* 102 (2) (2020) 023518. [arXiv:1907.07569](#).
 - [30] E. Abdalla, et al., Cosmology intertwined: A review of the particle physics, astrophysics, and cosmology associated with the cosmological tensions and anomalies, *JHEAp* 34 (2022) 49–211. [arXiv:2203.06142](#).
 - [31] R. V. Buniy, S. D. H. Hsu, Instabilities and the null energy condition, *Phys. Lett. B* 632 (2006) 543–546. [arXiv:hep-th/0502203](#).
 - [32] T. Qiu, Y.-F. Cai, X.-M. Zhang, Null Energy Condition and Dark Energy Models, *Mod. Phys. Lett. A* 23 (2008) 2787–2798. [arXiv:0710.0115](#).
 - [33] Y. Akrami, et al., Modified Gravity and Cosmology: An Update by the CANTATA Network, Springer, 2021. [arXiv:2105.12582](#).
 - [34] A. A. Starobinsky, A New Type of Isotropic Cosmological Models Without Singularity, *Phys. Lett. B* 91 (1980) 99–102.
 - [35] S. Capozziello, Curvature quintessence, *Int. J. Mod. Phys. D* 11 (2002) 483–492. [arXiv:gr-qc/0201033](#).
 - [36] A. De Felice, S. Tsujikawa, $f(R)$ theories, *Living Rev. Rel.* 13 (2010) 3. [arXiv:1002.4928](#).
 - [37] Y.-F. Cai, S. Capozziello, M. De Laurentis, E. N. Saridakis, $f(T)$ teleparallel gravity and cosmology, *Rept. Prog. Phys.* 79 (10) (2016) 106901. [arXiv:1511.07586](#).
 - [38] M. Krššák, E. N. Saridakis, The covariant formulation of $f(T)$ gravity, *Class. Quant. Grav.* 33 (11) (2016) 115009. [arXiv:1510.08432](#).
 - [39] M. Krssak, R. van den Hoogen, J. Pereira, C. Böhmer, A. Coley, Teleparallel theories of gravity: illuminating a fully invariant approach, *Class. Quant. Grav.* 36 (18)

- (2019) 183001. [arXiv:1810.12932](#).
- [40] S. Bahamonde, K. F. Dialektopoulos, C. Escamilla-Rivera, G. Farrugia, V. Gakis, M. Hendry, M. Hohmann, J. Levi Said, J. Mifsud, E. Di Valentino, Teleparallel gravity: from theory to cosmology, *Rept. Prog. Phys.* 86 (2) (2023) 026901. [arXiv:2106.13793](#).
- [41] J. Beltrán Jiménez, L. Heisenberg, T. Koivisto, Coincident General Relativity, *Phys. Rev. D* 98 (4) (2018) 044048. [arXiv:1710.03116](#).
- [42] L. Heisenberg, Review on $f(Q)$ gravity, *Phys. Rept.* 1066 (2024) 1–78. [arXiv:2309.15958](#).
- [43] J. Beltrán Jiménez, L. Heisenberg, T. S. Koivisto, S. Pekar, Cosmology in $f(Q)$ geometry, *Phys. Rev. D* 101 (10) (2020) 103507. [arXiv:1906.10027](#).
- [44] Y.-F. Cai, S.-H. Chen, J. B. Dent, S. Dutta, E. N. Saridakis, Matter Bounce Cosmology with the $f(T)$ Gravity, *Class. Quant. Grav.* 28 (2011) 215011. [arXiv:1104.4349](#).
- [45] T. Clifton, P. G. Ferreira, A. Padilla, C. Skordis, Modified Gravity and Cosmology, *Phys. Rept.* 513 (2012) 1–189. [arXiv:1106.2476](#).
- [46] S. Nojiri, S. D. Odintsov, V. K. Oikonomou, Modified Gravity Theories on a Nutshell: Inflation, Bounce and Late-time Evolution, *Phys. Rept.* 692 (2017) 1–104. [arXiv:1705.11098](#).
- [47] G.-B. Zhao, R. G. Crittenden, L. Pogosian, X. Zhang, Examining the evidence for dynamical dark energy, *Phys. Rev. Lett.* 109 (2012) 171301. [arXiv:1207.3804](#).
- [48] G.-B. Zhao, et al., Dynamical dark energy in light of the latest observations, *Nature Astron.* 1 (9) (2017) 627–632. [arXiv:1701.08165](#).
- [49] M. Cortés, A. R. Liddle, Interpreting DESI’s evidence for evolving dark energy (4 2024). [arXiv:2404.08056](#).
- [50] W. Giarè, M. A. Sabogal, R. C. Nunes, E. Di Valentino, Interacting Dark Energy after DESI Baryon Acoustic Oscillation measurements (2024). [arXiv:2404.15232](#).
- [51] K. V. Berghaus, J. A. Kable, V. Miranda, Quantifying Scalar Field Dynamics with DESI 2024 Y1 BAO measurements (4 2024). [arXiv:2404.14341](#).
- [52] Y. Tada, T. Terada, Quintessential interpretation of the evolving dark energy in light of DESI (4 2024). [arXiv:2404.05722](#).
- [53] I. J. Allali, A. Notari, F. Rompineve, Dark Radiation with Baryon Acoustic Oscillations from DESI 2024 and the H_0 tension (2024). [arXiv:2404.15220](#).
- [54] D. Wang, Constraining Cosmological Physics with DESI BAO Observations (2024). [arXiv:2404.06796](#).
- [55] E. O. Colgáin, M. G. Dainotti, S. Capozziello, S. Pourojaghi, M. M. Sheikh-Jabbari, D. Stojkovic, Does DESI 2024 Confirm Λ CDM? (2024). [arXiv:2404.08633](#).
- [56] Y. Carloni, O. Luongo, M. Muccino, Does dark energy really revive using DESI 2024 data? (2024). [arXiv:2404.12068](#).
- [57] A. G. Adame, et al., DESI 2024 III: Baryon Acoustic Oscillations from Galaxies and Quasars (2024). [arXiv:2404.03000](#).
- [58] A. G. Adame, et al., DESI 2024 IV: Baryon Acoustic Oscillations from the Lyman Alpha Forest (4 2024). [arXiv:2404.03001](#).
- [59] P. Mukherjee, N. Banerjee, Nonparametric reconstruction of interaction in the cosmic dark sector, *Phys. Rev. D* 103 (12) (2021) 123530. [arXiv:2105.09995](#).
- [60] P.-J. Wu, J.-Z. Qi, X. Zhang, Null test for cosmic curvature using Gaussian process*, *Chin. Phys. C* 47 (5) (2023) 055106. [arXiv:2209.08502](#).
- [61] X. Wang, G. Gu, X. Mu, S. Yuan, G.-B. Zhao, Dynamical dark energy in light of cosmic distance measurements II: a study using current observations (2024). [arXiv:2404.06310](#).
- [62] A. Shafieloo, A. G. Kim, E. V. Linder, Gaussian Process Cosmography, *Phys. Rev. D* 85 (2012) 123530. [arXiv:1204.2272](#).
- [63] Y.-F. Cai, M. Khurshudyan, E. N. Saridakis, Model-independent reconstruction of $f(T)$ gravity from Gaussian Processes, *Astrophys. J.* 888 (2020) 62. [arXiv:1907.10813](#).
- [64] X. Ren, T. H. T. Wong, Y.-F. Cai, E. N. Saridakis, Data-driven Reconstruction of the Late-time Cosmic Acceleration with $f(T)$ Gravity, *Phys. Dark Univ.* 32 (2021) 100812. [arXiv:2103.01260](#).
- [65] M. Aljaf, D. Gregoris, M. Khurshudyan, Constraints on interacting dark energy models through cosmic chronometers and Gaussian process, *Eur. Phys. J. C* 81 (6) (2021) 544. [arXiv:2005.01891](#).
- [66] J. Levi Said, J. Mifsud, J. Sultana, K. Z. Adami, Reconstructing teleparallel gravity with cosmic structure growth and expansion rate data, *JCAP* 06 (2021) 015. [arXiv:2103.05021](#).
- [67] A. Bonilla, S. Kumar, R. C. Nunes, S. Pan, Reconstruction of the dark sectors’ interaction: A model-independent inference and forecast from GW standard sirens, *Mon. Not. Roy. Astron. Soc.* 512 (3) (2022) 4231–4238. [arXiv:2102.06149](#).
- [68] R. C. Bernardo, J. Levi Said, A data-driven reconstruction of Horndeski gravity via the Gaussian processes, *JCAP* 09 (2021) 014. [arXiv:2105.12970](#).
- [69] X. Ren, S.-F. Yan, Y. Zhao, Y.-F. Cai, E. N. Saridakis, Gaussian processes and effective field theory of $f(T)$ gravity under the H_0 tension, *Astrophys. J.* 932 (2022) 2. [arXiv:2203.01926](#).
- [70] E. Elizalde, M. Khurshudyan, K. Myrzakulov, S. Bekov, Reconstruction of the quintessence dark energy potential from a Gaussian process (2022). [arXiv:2203.06767](#).
- [71] J. Liu, L. Qiao, B. Chang, L. Xu, Revisiting cosmography via Gaussian process, *Eur. Phys. J. C* 83 (5) (2023) 374.
- [72] J. A. S. Fortunato, P. H. R. S. Moraes, J. G. d. L. Júnior, E. Brito, Search for the $f(R, T)$ gravity functional form via gaussian processes, *Eur. Phys. J. C* 84 (2) (2024) 198. [arXiv:2305.01325](#).
- [73] Y. Yang, X. Ren, B. Wang, Y.-F. Cai, E. N. Saridakis, Data reconstruction of the dynamical connection function in $f(Q)$ cosmology (2024). [arXiv:2404.12140](#).
- [74] M. Seikel, C. Clarkson, M. Smith, Reconstruction of dark energy and expansion dynamics using Gaussian processes, *JCAP* 06 (2012) 036. [arXiv:1204.2832](#).
- [75] W. Hu, Crossing the phantom divide: Dark energy internal degrees of freedom, *Phys. Rev. D* 71 (2005) 047301. [arXiv:astro-ph/0410680](#).
- [76] M. Kunz, D. Sapone, Crossing the Phantom Divide, *Phys. Rev. D* 74 (2006) 123503. [arXiv:astro-ph/0609040](#).
- [77] Z.-K. Guo, Y.-S. Piao, X.-M. Zhang, Y.-Z. Zhang, Cosmological evolution of a quintom model of dark energy, *Phys. Lett. B* 608 (2005) 177–182. [arXiv:astro-ph/0410654](#).
- [78] X.-F. Zhang, H. Li, Y.-S. Piao, X.-M. Zhang, Two-field models of dark energy with equation of state across

- 1, *Mod. Phys. Lett. A* 21 (2006) 231–242. [arXiv:astro-ph/0501652](#).
- [79] M. Alimohammadi, L. Sadeghian, Quantum induced $w = -1$ crossing of the quintessence and phantom models, *JCAP* 01 (2009) 035. [arXiv:0806.0141](#).
- [80] Y.-f. Cai, M.-z. Li, J.-X. Lu, Y.-S. Piao, T.-t. Qiu, X.-m. Zhang, A String-Inspired Quintom Model Of Dark Energy, *Phys. Lett. B* 651 (2007) 1–7. [arXiv:hep-th/0701016](#).
- [81] D. Langlois, M. Mancarella, K. Noui, F. Vernizzi, Effective Description of Higher-Order Scalar-Tensor Theories, *JCAP* 05 (2017) 033. [arXiv:1703.03797](#).
- [82] D. Langlois, M. Mancarella, K. Noui, F. Vernizzi, Mimetic gravity as DHOST theories, *JCAP* 02 (2019) 036. [arXiv:1802.03394](#).
- [83] G. W. Horndeski, Second-order scalar-tensor field equations in a four-dimensional space, *Int. J. Theor. Phys.* 10 (1974) 363–384.
- [84] Y.-F. Cai, T. Qiu, Y.-S. Piao, M. Li, X. Zhang, Bouncing universe with quintom matter, *JHEP* 10 (2007) 071. [arXiv:0704.1090](#).
- [85] Y.-F. Cai, T. Qiu, R. Brandenberger, Y.-S. Piao, X. Zhang, On Perturbations of Quintom Bounce, *JCAP* 03 (2008) 013. [arXiv:0711.2187](#).
- [86] H.-H. Xiong, Y.-F. Cai, T. Qiu, Y.-S. Piao, X. Zhang, Oscillating universe with quintom matter, *Phys. Lett. B* 666 (2008) 212–217. [arXiv:0805.0413](#).
- [87] Y.-F. Cai, M. Li, X. Zhang, Emergent Universe Scenario via Quintom Matter, *Phys. Lett. B* 718 (2012) 248–254. [arXiv:1209.3437](#).
- [88] Y.-F. Cai, Y. Wan, X. Zhang, Cosmology of the Spinor Emergent Universe and Scale-invariant Perturbations, *Phys. Lett. B* 731 (2014) 217–226. [arXiv:1312.0740](#).
- [89] A. Ilyas, M. Zhu, Y. Zheng, Y.-F. Cai, Emergent Universe and Genesis from the DHOST Cosmology, *JHEP* 01 (2021) 141. [arXiv:2009.10351](#).
- [90] A. Vikman, Can dark energy evolve to the phantom?, *Phys. Rev. D* 71 (2005) 023515. [arXiv:astro-ph/0407107](#).
- [91] J. M. Cline, S. Jeon, G. D. Moore, The Phantom menaced: Constraints on low-energy effective ghosts, *Phys. Rev. D* 70 (2004) 043543. [arXiv:hep-ph/0311312](#).
- [92] F. W. Hehl, J. D. McCrea, E. W. Mielke, Y. Ne’eman, Metric affine gauge theory of gravity: Field equations, Noether identities, world spinors, and breaking of dilation invariance, *Phys. Rept.* 258 (1995) 1–171. [arXiv:gr-qc/9402012](#).
- [93] E. Gaztanaga, A. Cabre, L. Hui, Clustering of Luminous Red Galaxies IV: Baryon Acoustic Peak in the Line-of-Sight Direction and a Direct Measurement of $H(z)$, *Mon. Not. Roy. Astron. Soc.* 399 (2009) 1663–1680. [arXiv:0807.3551](#).
- [94] A. Oka, S. Saito, T. Nishimichi, A. Taruya, K. Yamamoto, Simultaneous constraints on the growth of structure and cosmic expansion from the multipole power spectra of the SDSS DR7 LRG sample, *Mon. Not. Roy. Astron. Soc.* 439 (2014) 2515–2530. [arXiv:1310.2820](#).
- [95] Y. Wang, et al., The clustering of galaxies in the completed SDSS-III Baryon Oscillation Spectroscopic Survey: tomographic BAO analysis of DR12 combined sample in configuration space, *Mon. Not. Roy. Astron. Soc.* 469 (3) (2017) 3762–3774. [arXiv:1607.03154](#).
- [96] C.-H. Chuang, Y. Wang, Modeling the Anisotropic Two-Point Galaxy Correlation Function on Small Scales and Improved Measurements of $H(z)$, $D_A(z)$, and $\beta(z)$ from the Sloan Digital Sky Survey DR7 Luminous Red Galaxies, *Mon. Not. Roy. Astron. Soc.* 435 (2013) 255–262. [arXiv:1209.0210](#).
- [97] C. Blake, et al., The WiggleZ Dark Energy Survey: Joint measurements of the expansion and growth history at $z < 1$, *Mon. Not. Roy. Astron. Soc.* 425 (2012) 405–414. [arXiv:1204.3674](#).
- [98] L. Anderson, et al., The clustering of galaxies in the SDSS-III Baryon Oscillation Spectroscopic Survey: baryon acoustic oscillations in the Data Releases 10 and 11 Galaxy samples, *Mon. Not. Roy. Astron. Soc.* 441 (1) (2014) 24–62. [arXiv:1312.4877](#).
- [99] G.-B. Zhao, et al., The clustering of the SDSS-IV extended Baryon Oscillation Spectroscopic Survey DR14 quasar sample: a tomographic measurement of cosmic structure growth and expansion rate based on optimal redshift weights, *Mon. Not. Roy. Astron. Soc.* 482 (3) (2019) 3497–3513. [arXiv:1801.03043](#).
- [100] R. Neveux, et al., The completed SDSS-IV extended Baryon Oscillation Spectroscopic Survey: BAO and RSD measurements from the anisotropic power spectrum of the quasar sample between redshift 0.8 and 2.2, *Mon. Not. Roy. Astron. Soc.* 499 (1) (2020) 210–229. [arXiv:2007.08999](#).
- [101] N. G. Busca, et al., Baryon Acoustic Oscillations in the Ly- α forest of BOSS quasars, *Astron. Astrophys.* 552 (2013) A96. [arXiv:1211.2616](#).
- [102] A. Font-Ribera, et al., Quasar-Lyman α Forest Cross-Correlation from BOSS DR11 : Baryon Acoustic Oscillations, *JCAP* 05 (2014) 027. [arXiv:1311.1767](#).
- [103] H. du Mas des Bourboux, et al., Baryon acoustic oscillations from the complete SDSS-III Ly α -quasar cross-correlation function at $z = 2.4$, *Astron. Astrophys.* 608 (2017) A130. [arXiv:1708.02225](#).